Biochimica et Biophysica Acta 1783 (2008) 2311–2322

Contents lists available at ScienceDirect

Biochimica et Biophysica Acta

journal homepage: www.elsevier.com/locate/bbamcr

SRC-dependent signalling regulates actin ruffle formation induced by glycerophosphoinositol 4-phosphate

Beatrice Maria Filippi [1], Stefania Mariggiò, Teodoro Pulvirenti [2], Daniela Corda *

Department of Cell Biology and Oncology, Consorzio Mario Negri Sud, Via Nazionale 8/A, 66030 Santa Maria Imbaro, Chieti, Italy

ARTICLE INFO

Article history:
Received 4 April 2008
Received in revised form 16 July 2008
Accepted 16 July 2008
Available online 3 August 2008

Keywords:
Glycerophosphoinositol
Phosphoinositide
Actin cytoskeleton
Signalling
Tyrosine kinase

ABSTRACT

The glycerophosphoinositols are diffusible phosphoinositide metabolites reported to modulate actin dynamics and tumour cell spreading. In particular, the membrane permeant glycerophosphoinositol 4-phosphate (GroPIns4*P*) has been shown to act at the level of the small GTPase Rac1, to induce the rapid formation of membrane ruffles. Here, we have investigated the signalling cascade involved in this process, and show that it is initiated by the activation of Src kinase. In NIH3T3 cells, exogenous addition of GroPIns4*P* induces activation and translocation of Rac1 and its exchange factor TIAM1 to the plasma membrane; in addition, in in-vitro assays, GroPIns4*P* favours the formation of a protein complex that includes Rac1 and TIAM1. Neither of these processes involves direct actions of GroPIns4*P* on these proteins. Thus, through the use of specific inhibitors of tyrosine kinases and phospholipase C (and by direct evaluation of kinase activities and inositol 1,4,5-trisphosphate production), we show that GroPIns4*P* activates Src, and as a consequence, phospholipase Cγ and Ca^{2+}/calmodulin kinase II, the last of which directly phosphorylates TIAM1 and leads to TIAM1/Rac1-dependent ruffle formation.

1. Introduction

Although the membrane phosphoinositides represent a minor, but essential, fraction of the total membrane phospholipids, they have crucial regulatory roles as docking molecules for protein-and lipid-binding domains [1–3] and as precursors of signalling molecules [4,5]. They are thus the substrates of different cellular enzymes, including lipid kinases, phosphatases and phospholipases, which catalyze the formation of active metabolites that are involved in the regulation of different cellular functions [6,7].

We have previously investigated the metabolism and physiological functions of a specific class of the phosphoinositide metabolites, the glycerophosphoinositols [7,8]. These are water-soluble products of phospholipase A_2 (PLA_2) and lysolipase activities that were originally identified in Ras-transformed epithelial cells [9], and were then characterized in a number of normal and transformed cell systems [7,10,11]. Recently, we have shown that in thyroid epithelial cells, the glycerophosphoinositols are specifically produced by a single enzyme, the PLA_2 IVα isoform, which possesses both PLA_2 and lysolipase activities [8]. In these cells, this pathway, and more specifically the formation of glycerophosphoinositol (GroPIns), is involved in the control of thyrotropin-independent cell proliferation [8]. In fibroblasts, glycerophosphoinositol 4-phosphate (GroPIns4*P*) has a role in promoting actin cytoskeleton reorganization, through the activation of the small GTPases of the Rho family [12]. Thus, in serum-starved Swiss 3T3 cells, exogenously added GroPIns4*P* stimulates the rapid formation of membrane ruffles, followed at later times by the formation of stress fibres [12]. This GroPIns4*P* effect in intact cells involves the activation of Rac1, as determined by an increased fraction of GTP-bound Rac1 and by a rapid translocation of green-fluorescent-protein (GFP)-tagged Rac1 into ruffles [12]. No information is available, however, on the mechanism by which GroPIns4*P* activates Rac1.

In addition to the effects reported above, GroPIns4*P* is involved in other processes in which cytoskeletal rearrangements are also essential, such as T-cell chemotaxis [13]. Through its ability to inhibit adenylyl cyclase activity [14], GroPIns4*P* enhances chemokine-induced chemotactic responses in Jurkat T-cells and in peripheral blood lymphocytes [13]. This GroPIns4*P* activity is due to the activation of the Rac1 guanine-nucleotide-exchange factor (GEF) Vav, which in turn regulates actin polymerization in these systems [13,15]. Moreover, when exogenously added to breast carcinoma and melanoma cell cultures, both GroPIns and GroPIns4*P* decrease the ability of these cells to degrade, and thus invade, the extracellular matrix, indicating the potential of these compounds in the control of tumour spreading [16].

Following on from the above, the present study was undertaken to define the molecular pathways involved in GroPIns4*P*-dependent ruffle formation in fibroblasts. This is relevant to the general remodelling of actin-based structures that are involved in

* Corresponding author. Tel.: +39 0872 570 353; fax: +39 0872 570412.
E-mail address: corda@negrisud.it (D. Corda).
[1] Current address: MRC Protein Phosphorylation Unit, College of Life Sciences, University of Dundee, Dundee, Scotland.
[2] Current address: Cell Biology Program, Sloan-Kettering Institute for Cancer Research, Memorial Sloan-Kettering Cancer Center, New York, NY 10021, USA.

0167-4889/$ – see front matter © 2008 Elsevier B.V. All rights reserved.
doi:10.1016/j.bbamcr.2008.07.021

processes such as cell adhesion, division and motility [17,18], and that are controlled by a number of signalling molecules and protein cofactors, including lipid kinases, serine/threonine and tyrosine kinases [19–22], phospholipases [23,24], scaffold proteins (such as IRSp53, filamin and Abl) [25–27], WASP family proteins [28] and the GTPases of the Rho family [29,30]. In addition, lipids, and more specifically the membrane phosphoinositides phosphatidylinositol 4,5-bisphosphate (PtdIns4,5P_2) and phosphatidylinositol 3,4,5-trisphosphate (PtdIns3,4,5P_3), have been shown to be relevant for actin cytoskeleton organization in three specific ways: (i) direct regulation of the activities and targeting of actin regulatory proteins, such as exchange factors, WASP family proteins and profilin [31–33]; (ii) stimulation of actin nucleation and the subsequent actin polymerization through the dissociation of capping proteins, such as CapZ and gelsolin, from the actin filaments [34]; and (iii) formation of cytoskeleton-plasma-membrane connections to form stable, bundled actin fibres [35,36].

Using biochemical and morphological approaches, we now show that GroPIns4*P* activates Src kinase, and thus initiates a phosphorylation cascade that leads to the activation of the specific GEF of Rac1, T-cell lymphoma invasion and metastasis protein-1 (TIAM1). This pathway is responsible for Rac1 activation, and finally for the formation of the membrane ruffles induced by GroPIns4*P*.

2. Materials and methods

2.1. Reagents

NIH3T3, HEK293T and SYF cells were from the American Type Culture Collection (ATCC, USA). Dulbecco's Modified Eagle's Medium (DMEM), OptiMEM, calf serum (CS), penicillin, streptomycin, trypsin-EDTA, L-glutamine and the Lipofectamine/plus reagent were from Gibco BRL (Grand Island, NY, USA). Foetal calf serum (FCS) was from Biochrom KG (Berlin, Germany). The TIAM1- and wild-type-Src-expressing constructs (see below) were kindly provided by I. Fleming (University of Dundee, Scotland, UK) and S. Gutkind (NIH, Bethesda, USA), respectively. The pEGFP-Rac1 was from our laboratory [12], while pEGFP was from Molecular Probes (Eugene, OR, USA). The constructs expressing the myc-tagged constitutively active forms of Rac1 (myc-L61Rac1), RhoA (myc-L63RhoA) and Cdc42 (myc-L61Cdc42) were kindly provided by A. Hall (Sloan-Kettering Institute for Cancer Research, NY, USA). TRITC- and FITC-labelled phalloidin were from Sigma-Aldrich (St. Louis, MO, USA), and Fluo3-AM and the Alexa 488-and Alexa 546-conjugated goat anti-rabbit and anti-mouse antibodies from Molecular Probes. For the antibodies: anti-HA was from Babco (Richmond, CA, USA), anti-p-Src (phosphorylated on tyrosine 416, p-Tyr416) from Upstate (Chicago, IL, USA), anti-PLCβ1, anti-PLCγ1, anti-TIAM1 (C-16), anti-c-Src were from Santa Cruz (Santa Cruz, CA, USA), the polyclonal anti-TIAM1 antibody was kindly provided by J.G. Collard (The Netherlands Cancer Institute), monoclonal anti-*c-myc* Cy3 conjugate clone 9E10 from Sigma-Aldrich and monoclonal antiphosphotyrosine clone 4G10 from Upstate. GroPIns4*P* was prepared by deacylation of phosphatidylinositol 4-phosphate (Avanti Polar Lipids, Alabaster, AL, USA), following [37]. KN-93, U73122, U73433, PP2, SU6656, GroPIns, mowiol and the secondary antibodies conjugated to horse-radish peroxidase and directed against mouse and rabbit IgGs were from Calbiochem (La Jolla, CA, USA). Ionomycin, ATP, genistein and 1,2-bis-(*o*-aminophenoxy)-ethane-*N*,*N*,-*N*',*N*'-tetraacetic acid tetraacetoxy-methyl ester (BAPTA-AM) were from Sigma-Aldrich. PDGF, CaMKII, Src, the "CaMKII activity assay" kit and the "Src assay kit" were from Upstate. The "D-myo-inositol 1,4,5-trisphosphate [^{3}H]-Biotrak assay system" and the ECL reagents were from Amersham Pharmacia (Piscataway, NJ, USA). [γ^{32}P]-ATP (3,000 Ci/mmole), Filter Count and Ultima Gold scintillation fluids were from Perkin Elmer Life Sciences (Boston, MA, USA). All other reagents were of the highest purities from standard commercial sources.

2.2. Cell culture, transfection and treatments

Cells were grown in DMEM supplemented with 2 mM glutamine, 100 U/ml penicillin, 0.1 mg/ml streptomycin, 10% CS (mouse fibroblasts, NIH3T3 cells) or FCS (human cell lines, HEK293T cells, mouse embryo fibroblasts, SYF cells). For immunofluorescence experiments, cells were seeded onto glass coverslips in 24-well plates at a concentration suitable for 70% confluence without transfection or 50% confluence in the case of Lipofectamine-based cell transfection. In the latter, about 24 h after seeding, NIH3T3 and SYF cells were transiently transfected with different plasmids (pEGFP-Rac1 encoding Rac1-GFP; pcDNA-C1199-TIAM1 encoding TIAM1-HA, pEGFP-C1199-TIAM1 encoding TIAM1-GFP, pRK5-L61Rac1 encoding myc-L61Rac1, pRK5-L63RhoA encoding myc-L63RhoA, pRK5-L61Cdc42 encoding myc-L61Cdc42 and pSM-c-Src encoding c-Src) with the Lipofectamine/plus reagent, following the manufacturer instructions. Before treatments, NIH3T3 and SYF cells were serum starved in DMEM with 2 mM glutamine, 1 U/ml penicillin and streptomycin for 24 h and with 0.1% FCS for 12 h, respectively. Then the cells were treated with the different stimuli and/or inhibitors, as indicated in the text and/or Figure legends.

2.3. Immunofluorescence analysis for membrane ruffling and protein localization

For ruffle assessment after treatments, the cells (NIH3T3 or SYF) were fixed with 4% (w/v) paraformaldehyde in PBS for 12 min, permeabilised in blocking solution (0.05% saponin, 0.5% BSA, 50 mM NH_4Cl, in PBS) for 20 min, and then incubated with 0.1 μg/ml TRITC- or FITC-labelled phalloidin for 45 min for filamentous actin visualization [12]. The samples (independent experiments in duplicate; 200 cells per sample) underwent blinded morphological scoring for ruffle formation, under an Axiophot microscope using a 100×1.3 objective (Carl Zeiss, Jena, Germany), as: absence, 0; partial response, 1; full response, 2 (see also [12]). This provided a maximum score of 400, with the data given as percentages of each response with respect to the respective control.

For protein localization, the effects of different agents were also analysed in NIH3T3 and SYF cells: the cells were fixed and permeabilized with blocking solution (see above), and then incubated with the specified primary and fluorescent-probe-(Alexa 488 or Alexa 546)-conjugated secondary antibody diluted in blocking solution and stained for actin (see above and [12]). To determine the specificity of GFP-tagged constructs, the same experiments were also performed with cells overexpressing GFP. This always showed a nuclear and cytoplasmic localization for GFP that did not change upon treatment. The samples were then analyzed with blinded quantification under an LSM 510 confocal microscope equipped with a 63× objective (Zeiss, Germany). Optical confocal sections were taken at 1 Airy unit with a resolution of 512×512 pixels and exported as TIFF files. The quantitative evaluation of the immuno-staining patterns was performed on at least 50 cells per sample, in at least three independent experiments, each in duplicate. The data are expressed as percentages of cells displaying a given pattern.

The endogenously expressed TIAM1 was also followed in NIH3T3 cells using a polyclonal anti-TIAM1 antibody kindly received from J.G. Collard (The Netherlands Cancer Institute) (see Results), however the high level of background labelling prevented a good resolution of the specific signal.

2.4. GroPIns4P-induced translocation of Rac1 and TIAM1, and Vav1 activation

For the membrane translocation of Rac1 and TIAM1, NIH3T3 cells were serum starved in DMEM with 2 mM glutamine, 1 U/ml penicillin and 0.1 mg/ml streptomycin for 24 h, stimulated, lysed and processed

as previously reported [38]. For Vav1 activation, the cells were treated as previously reported [13].

2.5. TIAM1-HA pull-down assay

Cell lysates (30 μg/μl) were prepared from HEK293T cells over-expressing TIAM1-HA [39]. The cells were lysed in 25 mM Tris–HCl, pH 7.6, 100 mM NaCl, 10 mM $MgCl_2$, 1% glycerol and 1% NP-40, and then centrifuged at 90,000 ×g for 30 min at 4 °C. Ten microliters of the supernatant were diluted (1:15) in reaction buffer (25 mM Tris-HCl, pH 7.6, 100 mM NaCl, 10 mM $MgCl_2$), and cleared with 50% glutathione resin for 1 h at 4 °C on a rotating wheel, and then incubated for 10 min at 37 °C with 50 μM GroPIns4*P*. Finally, 4 μg purified Rac1-GST or purified GST [12], 10 μl 50% glutathione resin and 20 μl 2 mg/ml BSA (final volume 200 μl) were added, and the samples were incubated for 1 h at 4 °C on a rotating wheel. The pellets were recovered by centrifugation at 800 ×g for 6 min at 4 °C, and after 3 washes with reaction buffer they were analyzed by immuno-blotting with the anti-TIAM1 antibody. The amount of TIAM1-HA co-immunoprecipitated with Rac1-GST was quantified by the NIH imaging programme (densitometric analysis).

2.6. CaMKII activity assay

NIH3T3 cells were plated at 3.5×10^5 cells/well in 6-well plates, and the day after they were starved in DMEM, 0.1% BSA. After 20 h starvation, the cells were stimulated with 50 μM GroPIns4*P* or 10 ng/ml PDGF. After treatments, the cells were harvested, lysed with 30 passes through a 27-gauge needle in 20 mM MOPS, pH 7.5, 25 mM β-glycerophosphate, 1 mM Na_3VO_4, 1 mM DTT with protease inhibitors (0.5 μg/ml leupeptin, 2 μg/ml aprotinin, 0.5 mM phenanthroline, 2 μM pepstatin and 1 mM PMSF), and centrifuged at 2,000 ×g for 3 min at 4 °C. The CaMKII enzymatic activity was measured with the "CaMKII activity assay" kit (Upstate) [40], either in the absence (final 5 mM EGTA) or presence (final 2 mM $CaCl_2$) of Ca^{2+}. The same assay was also performed using purified CaMKII. Here, 0.25 μg purified CaMKII was incubated with 50 μM GroPIns4*P*, and then the CaMKII activity was carried out following the same procedure described above.

2.7. $[Ca^{2+}]_i$ measurements

NIH3T3 cells were loaded with 4 μM Fluo3-acetoxymethyl ester (Fluo3-AM) in HEPES-buffered saline solution (10 mM HEPES, pH 7.0,

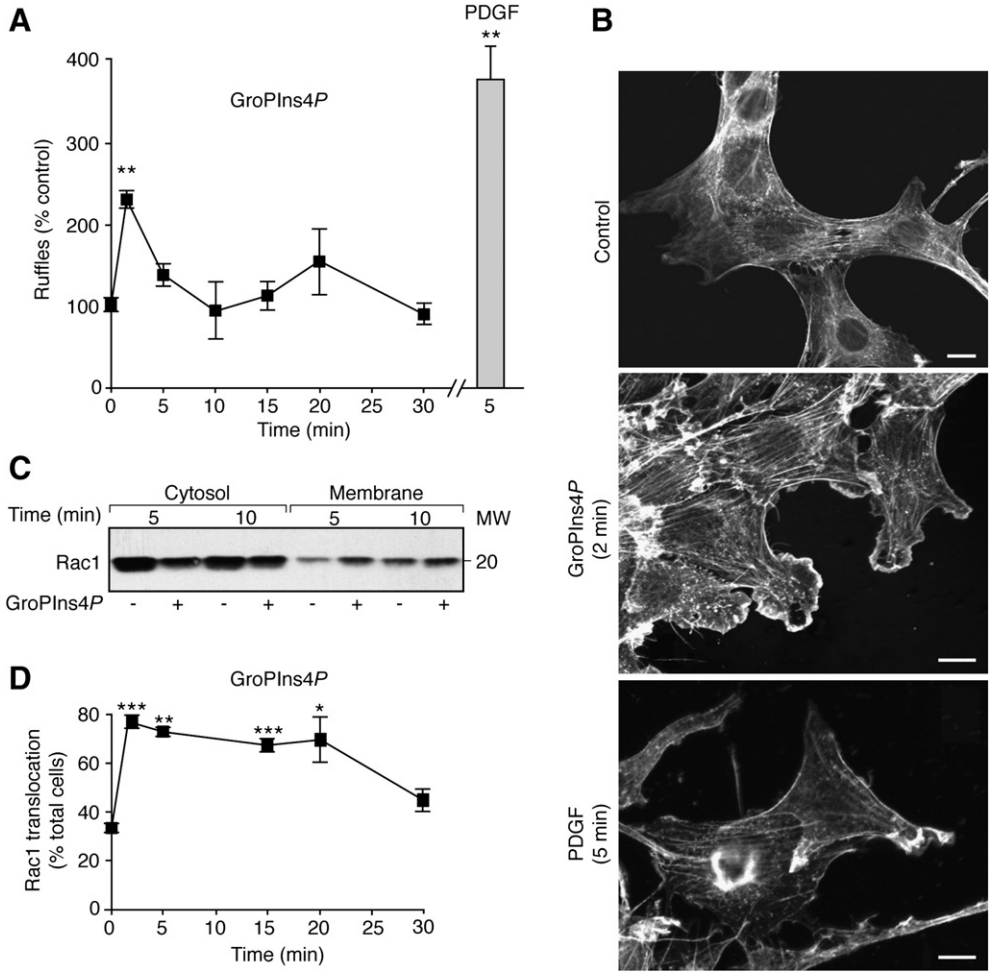

Fig. 1. GroPIns4*P*-dependent ruffle formation and Rac1 translocation to the plasma membrane. Serum-starved NIH3T3 cells were treated with 50 μM GroPIns4*P* or 10 ng/ml PDGF for the indicated times. Fixed cells were stained with FITC-labelled phalloidin and analyzed by confocal microscopy. (A) Quantification of ruffle formation, as indicated in Materials and methods and [12]. Data are expressed as percentages of the unstimulated control for each time point, as means (±s.d.) of three independent experiments, each in duplicate. (B) Representative confocal images of actin staining, as indicated. Scale bars: 10 μm. (C) Representative Western blot showing endogenous Rac1 localization in the cytosolic and membrane fractions. MW, molecular-weight markers (kDa). (D) Quantification of Rac1-GFP translocation to the plasma membrane in cells overexpressing Rac1-GFP and treated as indicated. The quantitative evaluation of the immuno-staining patterns was performed on at least 50 cells per sample (see Materials and methods). Data are expressed as percentages of total cells showing plasma-membrane localization of Rac1-GFP, as means (±s.d.) of at least three independent experiments, each in duplicate. Statistical significance: $^*P<0.05$, $^{**}P<0.01$, $^{***}P<0.001$, compared to untreated sample (paired Student's *t* test).

137 mM NaCl, 5 mM KCl, 4 mM $MgCl_2$, 3 mM $CaCl_2$ and 25 mM glucose) for 30 min at 37 °C, as previously described [41]. The fluorescence measurements were carried out in the HEPES-buffered saline solution under an IX70 microscope (Olympus, Hamburg, Germany) equipped with a TILL Photonics imaging system (Gräfelfing, Germany). The cells were scanned for at least 30 s to establish baseline fluorescence and to check for spontaneous $[Ca^{2+}]_i$ rises, then movies were taken over 8 min following the addition of 50 μM GroPIns4*P* and the other stimuli (see text and Fig. 6). The various inhibitors were applied before the stimulation.

Image analysis: Cells were selected at random and the fluorescence of each frame was calculated by the TILL Photonics imaging system. After background subtraction, fluorescence values were plotted as increases in fluorescence per second. The estimation of Fluo3-AM fluorescence intensity (representative of $[Ca^{2+}]_i$) was reported as the pseudo-ratio (ΔF/F0) (see Table 2 and references herein).

2.8. $InsP_3$ measurements

NIH3T3 cells were plated at 3.5×10^5 cell/well in 6-well plates, and the day after they were serum starved. After 20 h of starvation, the cells were stimulated in DMEM plus 20 μM LiCl at 37 °C for 2 min to 15 min with 50 μM GroPIns4*P*, 5 I.U./ml thrombin, 10 ng/ml PDGF or 100 μM ATP. For the experiments performed with cell homogenates, the NIH3T3 cells were harvested and lysed by 30 passes through a 27-gauge needle, in a buffer containing 20 mM HEPES, pH 7.4, 3 mM EGTA, 0.2 mM EDTA, 0.83 mM $MgCl_2$, 1.5 mM $CaCl_2$, 20 mM NaCl, 30 mM KCl, 1 mM DTT, 20 mM LiCl and protease inhibitors. Then these

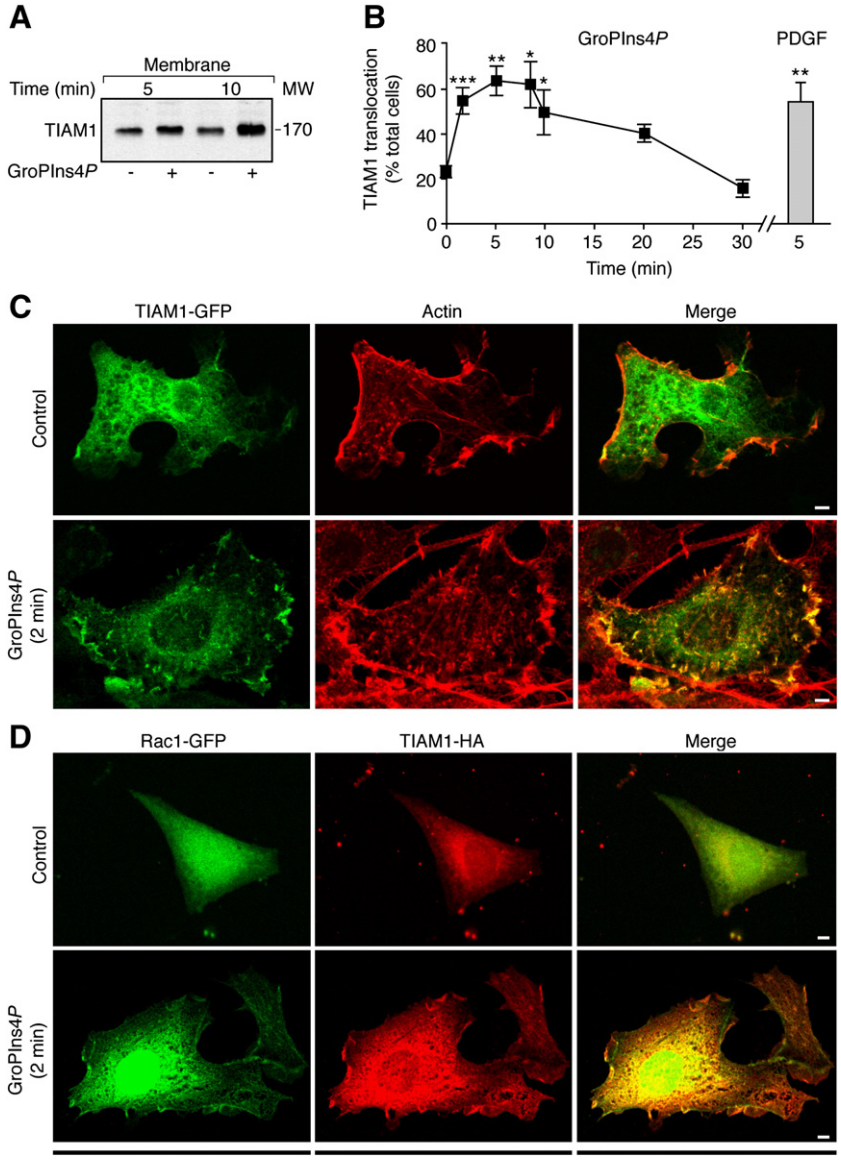

Fig. 2. GroPIns4*P*-dependent translocation of TIAM1 and Rac1 to the plasma membrane. Serum-starved NIH3T3 cells not transfected (A), overexpressing TIAM1-GFP alone (B and C) or TIAM1-HA and Rac1-GFP (D) were treated with 50 μM GroPIns4*P* or 10 ng/ml PDGF for the indicated times. (A) Representative Western blot showing endogenous TIAM1 localization in the membrane fractions. MW, molecular-weight marker (kDa). For the panels reporting immunofluorescence data (B-D), fixed cells were stained with TRITC-labelled phalloidin (B and C) or the anti-HA antibody (D), and analyzed by confocal microscopy. (B) Quantification of TIAM1-GFP localization at the plasma membrane. The quantitative evaluation of the immuno-staining patterns was performed on at least 50 cells per sample (see Materials and methods). Data are expressed as percentages of cells with plasma-membrane localization of TIAM1-GFP, as means (±s.d.) of four independent experiments, each in duplicate. (C) Representative confocal images of TIAM1-GFP localization (green) and actin staining (red), as indicated. Scale bars, 5 μm. (D) Representative confocal images of Rac1-GFP (green) and TIAM1-HA (red) localization, as indicated. Scale bars: 5 μm. Statistical significance: $*P<0.05$, $**P<0.01$, $***P<0.001$, compared to untreated sample (paired Student's *t* test).

homogenates (400 μg/sample) were treated as described above. The incubations with the indicated compounds were stopped by addition of 20% perchloric acid, and the InsP_3 levels were determined using the "D-myo-inositol 1,4,5-trisphosphate [^{3}H] - Biotrak assay system" (Amersham Pharmacia). With the cell homogenates, the anti-PLCβ and anti-PLCγ antibodies (20 μg/ml) [42] were added prior to stimulation.

2.9. Src activation assay

NIH3T3 cells were plated into 6-well dishes (3.5×10^5 cells/well). The day after, the cells were serum starved for 20 h and then stimulated with 50 μM GroPIns4*P* and 10 ng/ml PDGF. After this treatment, the cells were lysed in buffer containing 60 mM Tris–HCl, pH 7.4, 30 μM β-glycerophosphate, 50 μM β-mercaptoethanol, 1 mM Na_3VO_4, 2% SDS, 10% glycerol and protease inhibitors (as above) and processed for SDS-PAGE and Western blotting with anti-p-Src (p-Tyr416) and anti-c-Src antibodies. The extent of Src phosphorylation was evaluated using an NIH imaging system and normalised for the amounts of total Src. Across the repeated independent experiments, data are given as percentages of each response with respect to the relevant control. The assay with the purified Src was performed with NIH3T3 cells lysed with 30 passes through a 27-gauge needle in a buffer containing 60 mM Tris–HCl, pH 7.4, 30 μM β-glycerophosphate, 50 μM β-mercaptoethanol, 1 mM Na_3VO_4, 2% SDS, 10% glycerol and protease inhibitors, followed by centrifugation at 2000 ×g for 3 min at 4 °C. Thus, 0.25 μg purified Src was incubated with 50 μM GroPIns4*P* in the absence and presence of 200 μg NIH3T3 cell lysate, with Src activation measured using the commercial "Src assay kit" kit (Upstate).

2.10. Statistical analysis

All experiments are presented as means of duplicate or triplicate determinations, which were repeated at least three times. Statistical analysis was carried out using the paired Student's *t* test.

3. Results

3.1. GroPIns4P triggers ruffle formation and Rac1 translocation to the plasma membrane in NIH3T3 cells

In NIH3T3 cells, the addition of GroPIns4*P* (at 50 μM, unless otherwise specified) induced a rapid increase in ruffle formation, to a level 2.5-fold the control (within 2 min), which decreased to some 140% of control after 5 min, as detected by immunofluorescence analyses (Fig. 1A, B and Materials and methods). This effect of GroPIns4*P* was dose dependent, from around 10% stimulation at 1 μM to a maximal response at 50 μM, as has also been seen in Swiss 3T3 fibroblasts [12]. Longer times of exposure to GroPIns4*P* (15–20 min) led to the formation of stress fibres in both of these cell systems (Beatrice Maria Filippi, unpublished data) [12]; whereas a 5 min treatment with PDGF (10 ng/ml; used as a positive control in all experiments) produced an increase in ruffles to a level 3.8-fold the control, with the appearance of circular dorsal waves (circular ruffles) [43] (Fig. 1A and B).

Western blotting revealed that the GroPIns4*P*-induced formation of membrane ruffles was associated with the activation (evaluated by affinity precipitation of GTP-bound Rac1, data not shown and [12]) and translocation of endogenous Rac1 from the cytosolic fraction to the membrane fraction (Fig. 1C). This was confirmed by following the translocation of overexpressed Rac1-GFP to the plasma membrane by immunofluorescence (Fig. 1D; Supplementary Information, Figure S1 and S2). This translocation occurred in 75% of the stimulated cells (which represented a level 2.3-fold the control, as revealed by blinded scoring; Fig. 1D and Materials and methods).

As a control, the constitutively active forms of Rac1 (L61Rac1), RhoA (L63RhoA) and Cdc42 (L61Cdc42) were overexpressed in NIH3T3 cells and the rearrangements of the actin cytoskeleton were monitored (see Materials and methods and Supplementary Information, Figure S3). The ruffles (and stress fibres) formed under these conditions were reminiscent of those present in GroPIns4*P*-stimulated cells, whereas no filopodia were observed upon GroPIns4*P* stimulation (Fig. 1B and Supplementary Information, Figure S3).

3.2. GroPIns4P-dependent Rac1 activation and ruffle formation requires TIAM1

To determine the molecular mechanisms of this GroPIns4*P*-dependent Rac1 activation and translocation to the plasma membrane, we looked for the specific GEF involved in this process. In Jurkat T-cells GroPIns4*P* induces Rac1 stimulation by increasing the phosphorylation level and activation of the exchange factor Vav [13]; in contrast, in NIH3T3 cells treated with GroPIns4*P*, no modification of Vav1 phosphorylation was detected (data not shown). The possibility that GroPIns4*P* could activate Vav3 (known to be expressed at low levels in NIH3T3 cells, [44,45]) was also excluded based on the observation that this GEF acts also on Cdc42, inducing filopodia formation, an effect never detected upon GroPIns4*P* addition [12].

Among the other GEFs that can act on Rac1, we then investigated TIAM1, since it is expressed in NIH3T3 cells and it is known to be specifically involved in Rac1-dependent ruffle formation [46]. Western blotting indicated that in parallel with Rac1, endogenous TIAM1 was also enriched in the membrane fraction upon GroPIns4*P* stimulation (Fig. 2A). As endogenous TIAM1 could not be followed by immunofluorescence of intact cells due to the lack of suitable antibodies (see Materials and methods) [47], serum-starved NIH3T3 cells overexpressing TIAM1-GFP (see Materials and methods) were stimulated with GroPIns4*P*. Under these conditions, TIAM1-GFP was seen to translocate to the plasma membrane in 55% of the cells within 2 min (reaching a level 2.5-fold the control; Fig. 2B and Materials and methods); this was maintained for up

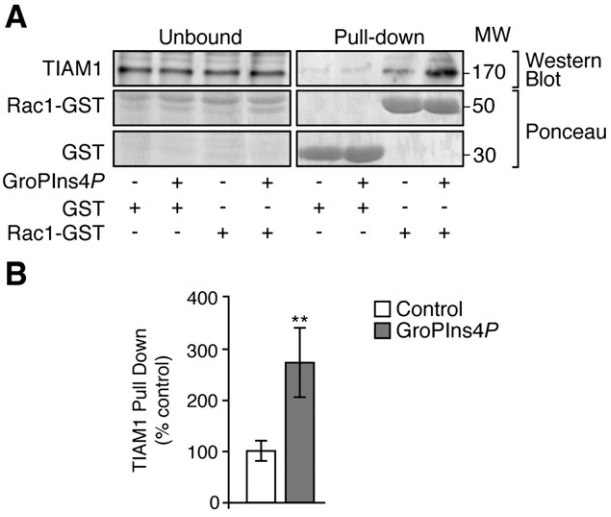

Fig. 3. Rac1-GST pull-down assay from lysates of TIAM1-overexpressing cells. Lysates from HEK293T cells overexpressing TIAM1-HA (120 μg) were diluted, pre-cleared and incubated with 50 μM GroPIns4*P* for 10 min at 37 °C (see Materials and methods). Finally, 4 μg purified Rac1-GST or GST alone, 10 μl glutathione resin and 200 μg/ml BSA were added, and the samples incubated for 1 h at 4 °C on a rotating wheel. Bound proteins were separated by centrifugation, as reported in the Materials and methods. A fraction of the supernatant (Unbound, panel A on the left) and the resins with the bound proteins (Pull-down, panel A on the right) were recovered and analysed by SDS-PAGE and Western blotting. The figure shows the Ponceau staining of the blots as loading control and the immuno-blotting with the anti-TIAM1 antibody (see Materials and methods). MW, molecular-weight markers (kDa). (B) Quantification of TIAM1 co-precipitated with Rac1-GST by densitometric analysis with the NIH Image programme. Data are expressed as percentages of unstimulated control, as means (±s.d.) of four independent experiments, each in duplicate. Statistical significance: $^{**}P<0.01$, compared to untreated sample (paired Student's *t* test).

to 10 min and was comparable to the PDGF stimulation (Fig. 2B). In addition, TIAM1-GFP co-localized with actin, indicating its association with membrane ruffles (Fig. 2C). By 30 min of GroPIns4*P* treatment, TIAM1 was completely redistributed back into the cytosol (Fig. 2B).

To directly evaluate whether this GroPIns4*P* action is exerted at the level of the interaction between TIAM1 and Rac1, immunofluorescence assays were performed in NIH3T3 cells overexpressing both Rac1-GFP and TIAM1-HA (see Materials and methods). Within 2 min of GroPIns4*P* addition to cells, translocation to the same plasma-membrane structures of both Rac1-GFP and TIAM1-HA was seen (Fig. 2D), which persisted for up to 20 min (data not shown), in line with the translocation of the individual proteins shown above (Figs. 1C and D, 2A and B). GroPIns4*P* also increased the interaction between TIAM1 and Rac1 to a level 2.8-fold the control when added to in-vitro pull-down experiments performed with purified Rac1-GST and lysates of HEK293T cells overexpressing TIAM1-HA (Fig. 3 and Materials and methods).

These data indicate that GroPIns4*P* induces the interaction of Rac1 and TIAM1 and their co-localization at the site of membrane ruffle formation at the plasma membrane.

3.3. Ca^{2+}/calmodulin kinase II is involved in GroPIns4P-dependent ruffle formation

The data reported above are consistent with the hypotheses that GroPIns4*P* is either acting by directly binding to, and favouring the formation of, the TIAM1/Rac1 complex, or that as with PDGF, GroPIns4*P* acts on one of the signalling enzymes upstream of TIAM1 activation. The latter possibility was analyzed by investigating the contributions of a number of known TIAM1 regulators. This initially led to the exclusion of phosphoinositide 3-kinase, as indicated by using the inhibitor wortmannin with GroPIns4*P*-induced membrane ruffles (Beatrice Maria Filippi, unpublished data and [12]). We then analysed Ca^{2+}/calmodulin kinase II (CaMKII), which is known to phosphorylate TIAM1 on threonine residues, thus favouring TIAM1 translocation to the plasma membrane [38,48]. In serum-starved cells treated with a CaMKII-specific inhibitor (20 μM KN-93, which results in a complete inhibition of CaMKII enzymatic activity) [49,50], the GroPIns4*P* effect on ruffle formation was completely blocked (Table 1). In parallel, PDGF stimulation of ruffle formation underwent a 60% inhibition with KN-93, while the phorbol ester phorbol 12-myristate 13-acetate (PMA), which induces ruffle formation in a CaMKII-independent manner by activating protein kinase C (PKC) [51,52], was not inhibited by KN-93 (Table 1).

Table 1
Ruffle formation in NIH3T3 cells

	No pretreatment	Pretreatments (% unstimulated control)				
		KN-93	SU6656	PP2	U-73122	U-73433
Unstimulated (absolute scores)[a]	100±12 (54±31)	100±15 (37±8)	100±23 (115±20)	100±3 (121±34)	100±52 (7±5)	100±17 (34±9)
GroPIns4*P*	247±57**	72±24	13±30*	140±20*	162±22*	200±25**
PDGF	378±116**	149±24*	163±42*	220±19**	245±165**	350±3***
PMA	193±55**	194±19*	nd	nd	nd	nd

Serum-starved NIH3T3 cells were pretreated with 20 μM KN-93 (CaMKII inhibitor; 24 h), 10 μM SU6656 (Src inhibitor; 10 min), 10 μM PP2 (Src inhibitor; 10 min), 5 μM U-73122 (PLC inhibitor; 10 min) or 5 μM U-73433 (inactive analogue of PLC inhibitor; 10 min), and then stimulated with 50 μM GroPIns4*P* (2 min), 10 ng/ml PDGF (5 min) or 10 μM PMA (5 min). Fixed cells were stained with TRITC-labelled phalloidin and subjected to blinded morphological scoring for ruffle formation (see Materials and methods). Data are given as percentages of each response with respect to their relevant control, as means (±s.d.) of at least three independent experiments, each performed in duplicate. The 100% refers to the unstimulated sample and represents the amount of cells presenting membrane ruffles under basal conditions. GroPIns4*P*, glycerophosphoinositol 4-phosphate; PMA, phorbol 12-myristate 13-acetate.
Statistical significance: *$P<0.05$, **$P<0.01$, ***$P<0.001$, compared to the respective untreated sample (paired Student's *t* test). nd, not determined.
[a] In parentheses: absolute ruffle quantification score obtained by counting 200 cells per sample. Each 100% value of the unstimulated samples refers to its corresponding score.

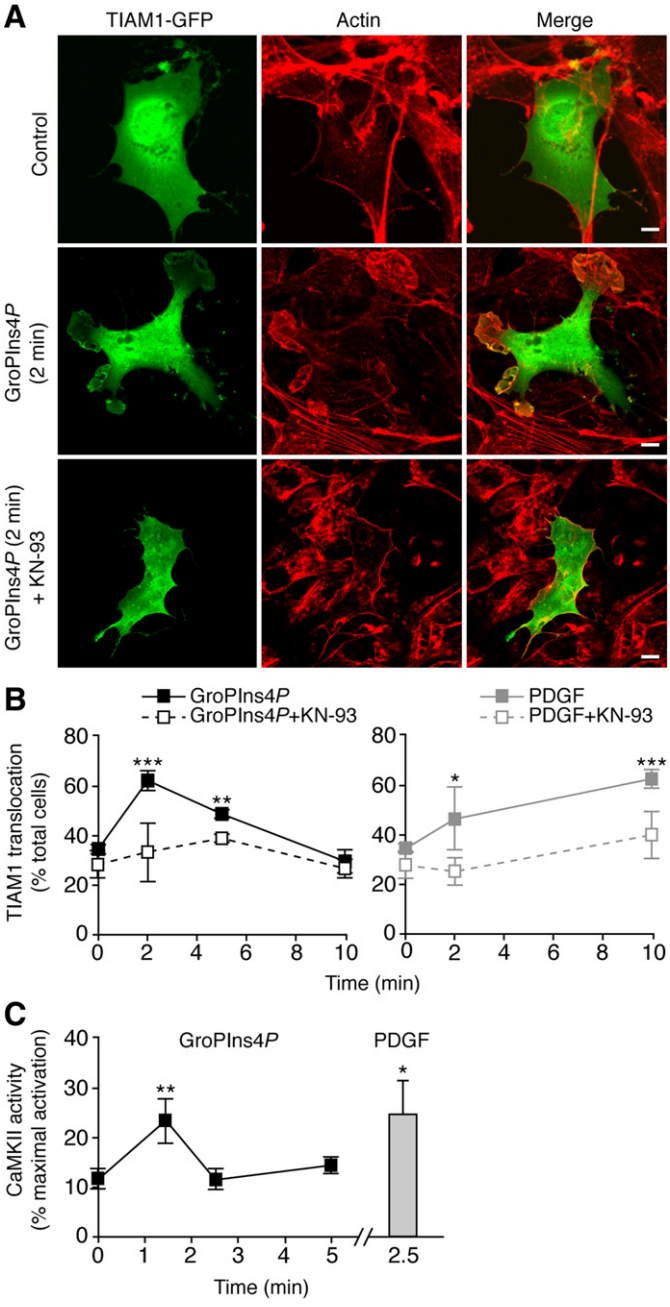

Fig. 4. CaMKII activity is necessary for GroPIns4*P* effects in NIH3T3 cells. Serum-starved NIH3T3 cells with (A and B) or without (C) overexpression of TIAM1-GFP were pretreated in the absence (A–C) or presence (A and B) of 20 μM KN-93 (CaMKII inhibitor; 24 h, during serum starvation) and stimulated with 50 μM GroPIns4*P* or 10 ng/ml PDGF for the indicated times. (A) Cells were fixed and stained with TRITC-labelled phalloidin and analyzed by confocal microscopy. Representative confocal images of TIAM1-GFP localization (green) and actin staining (red), as indicated. Scale bars: 10 μm. (B) Quantification of TIAM1-GFP localization at the plasma membrane, as indicated (see Materials and methods). Data are expressed as percentages of total cells with plasma-membrane localization of TIAM1-GFP, as means (±s.d.) of four independent experiments, each in duplicate. (C) Cell homogenates were assayed for CaMKII activation, as indicated (see Materials and methods). Data are expressed as percentages of maximum activation when cells were lysed in the presence of 2 mM Ca^{2+}, as means (±s.d.) of three independent experiments, each in duplicate. Statistical significance: *$P<0.05$, **$P<0.01$, ***$P<0.001$, compared to untreated sample (paired Student's *t* test).

The CaMKII inhibitor was also used in immunofluorescence experiments analyzing TIAM1-GFP localization. In line with the data reported above on ruffle formation (Table 1), KN-93 completely inhibited the effects of both GroPIns4*P* and PDGF on TIAM1-GFP

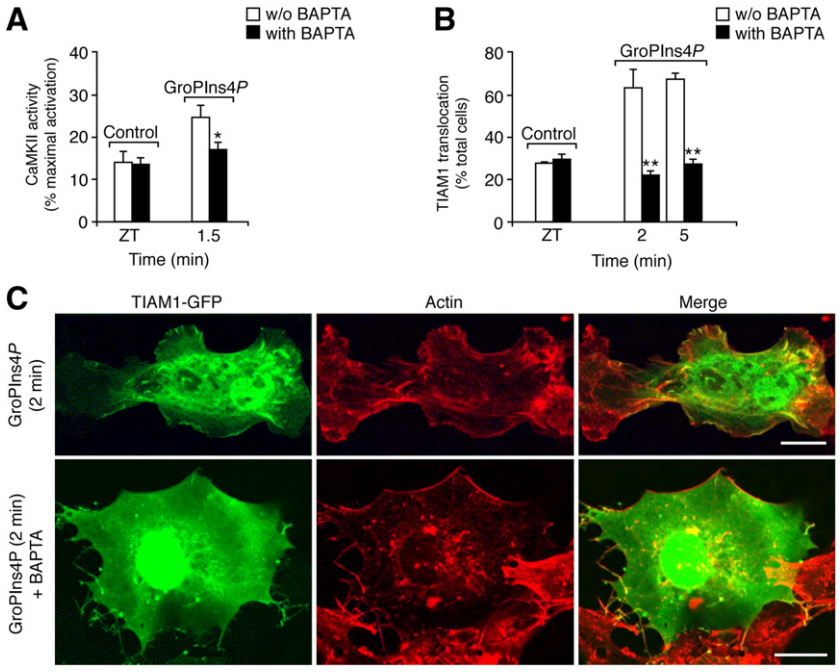

Fig. 5. BAPTA-AM block of GroPIns4*P*-dependent CaMKII activation and TIAM1 translocation to the plasma membrane. Serum-starved NIH3T3 cells without (A) or with (B and C) overexpression of TIAM1-GFP were pretreated in the absence or presence of 20 μM BAPTA-AM (Ca^{2+}chelator; 30 min, at the end of serum starvation) and stimulated with 50 μM GroPIns4*P* for the indicated times. (A) Cells were assayed for CaMKII activation as indicated. Data are expressed as percentages of maximum activation when cells were lysed in the presence of 2 mM Ca^{2+}, as means (±s.d.) of three independent experiments, each in duplicate. ZT, zero time unstimulated control. (B) Quantification of TIAM1-GFP localization at the plasma membrane, as indicated (see Materials and methods). Data are expressed as percentages of total cells with plasma-membrane localization of TIAM1-GFP, as means (±s.d.) of two independent experiments, each in duplicate. ZT, zero time unstimulated control. (C) Representative confocal images of TIAM1-GFP localization (green) and actin staining (red), as indicated. Scale bars: 10 μm. Statistical significance: $*P<0.05$, $**P<0.001$ compared to the respective ZT samples without BAPTA-AM pretreatment (paired Student's *t* test).

translocation to the plasma membrane (Fig. 4A and B). These data are consistent with CaMKII being part of the signalling of GroPIns4*P*-induced TIAM1 membrane translocation and ruffle formation.

Indeed, in intact cells, GroPIns4*P* activated the CaMKII enzymatic activity (see Materials and methods) in a rapid (within 1.5 min) and transient manner, with a maximal 100% increase (over untreated samples), as also seen for PDGF (Fig. 4C). With GroPIns4*P*, the CaMKII activity then returned to basal levels within 2.5 min (Fig. 4C). However, GroPIns4*P* did not directly stimulate CaMKII activity, since when purified CaMKII was used in these assays, no effects of GroPIns4*P* were detected (the purified CaMKII basal activity was 4.10 ±0.49 pmol phosphate incorporated into the substrate peptide/min; see Materials and methods).

GroPIns4*P*-dependent activation of CaMKII could involve modulation of intracellular calcium concentrations ($[Ca^{2+}]_i$), as Ca^{2+} is required together with calmodulin for CaMKII enzymatic activity [53]. CaMKII activity assays were thus performed after chelating $[Ca^{2+}]_i$ with the calcium chelator BAPTA-AM [50]. When NIH3T3 cells were

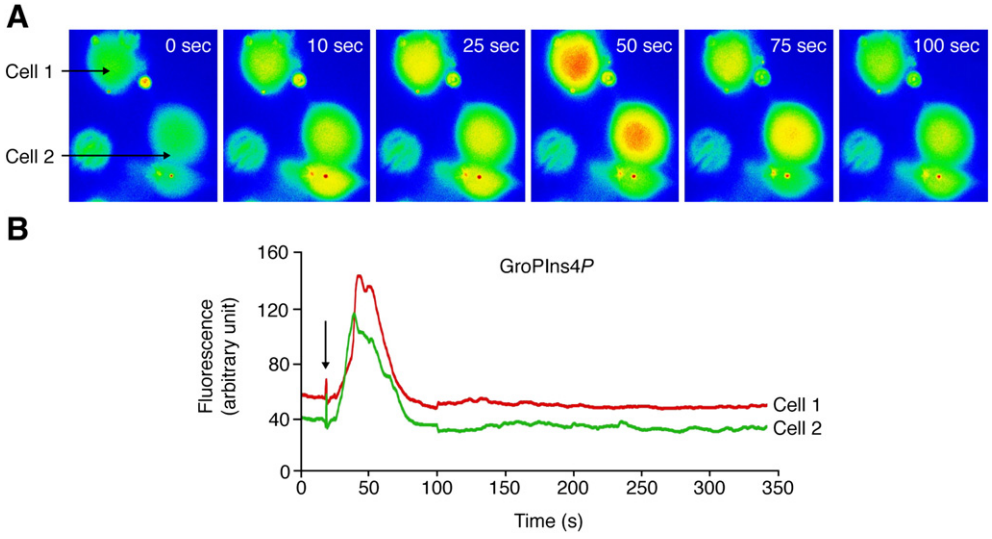

Fig. 6. GroPIns4*P*-induced $[Ca^{2+}]_i$ increases in NIH3T3 cells. Cells were loaded with 4 μM Fluo3-AM (30 min), washed, and then treated with 50 μM GroPIns4*P* and monitored for $[Ca^{2+}]_i$ increases (see Materials and methods). (A) Selected frames within 100 s (*sec*) from a representative time-lapse movie showing the colour-coded intensities representing $[Ca^{2+}]_i$ (green, low; red, high) after addition of 50 μM GroPIns4*P*. (B) Quantification of the kinetics of $[Ca^{2+}]_i$ increase stimulated by 50 μM GroPIns4*P* in the two cells in (A) (*Cell 1*, *Cell 2*). Data are expressed as fluorescence values calculated by the Till Photonic software (see Materials and methods; arbitrary units). The arrow indicates the addition of GroPIns4*P*.

pretreated with 20 μM BAPTA-AM for 30 min, the subsequent addition of GroPIns4*P* did not elicit the expected activation of CaMKII (Fig. 5A). This indicates that GroPIns4*P* requires an increase in $[Ca^{2+}]_i$ to activate CaMKII.

In parallel, immunofluorescence experiments in TIAM1-GFP-over-expressing NIH3T3 cells pretreated with BAPTA-AM and stimulated with GroPIns4*P* did not show any translocation of TIAM1-GFP to the plasma membrane or any ruffle formation (Fig. 5B and C).

In summary, $[Ca^{2+}]_i$ and CaMKII mediate the activation and translocation of TIAM1 to the plasma membrane induced by GroPIns4*P*.

3.4. GroPIns4P modulates intracellular Ca^{2+} concentrations through phospholipase Cγ activation

The requirement for GroPIns4*P*-dependent increases in $[Ca^{2+}]_i$ prompted us to analyze the mechanisms involved in this process. To this end, we monitored $[Ca^{2+}]_i$ by cell imaging in NIH3T3 cells loaded with the calcium-probe Fluo3-AM (see Materials and methods). These cells were then treated with GroPIns4*P* (from 1 μM to 50 μM), and/or with the controls of PDGF (10 ng/ml), ATP (100 μM) and ionomycin (10 μM) (Fig. 6). The $[Ca^{2+}]_i$ increases induced by GroPIns4*P* were rapid (maximal within 25 s) and transient (persisting for up to 50 s) (Fig. 6A and B). Table 2 provides a summary of the $[Ca^{2+}]_i$ levels (see also Materials and methods) stimulated by GroPIns4*P* and a range of further pretreatments in both the absence and the presence of specific enzyme inhibitors (see also below). As indicated, GroPIns4*P* produced a pronounced increase in Fluo3-AM fluorescence in about 60% of the cells analyzed per sample, well in line with the effects of ATP and PDGF

Table 2
Quantification of $[Ca^{2+}]_i$ in NIH3T3 cells

	Pretreatments	ΔF/F0	% of cells
Control	w/o	0.06±0.16	2.5±8
GroPIns4*P*	w/o	1.08±0.14***	58±3
PDGF	w/o	0.94±0.08***	65±9
ATP	w/o	1.52±0.09***	82±3
Ionomycin	w/o	1.33±0.16***	96±1
GroPIns	w/o	0.06±0.03	0
GroPIns4*P*	EGTA	0.94±0.13***	81±6
GroPIns4*P*	U-73122	0.05±0.01	0
PDGF	U-73122	0.08±0.06	0
ATP	U-73122	0.07±0.10	0
GroPIns4*P*	U-73443	1.1±0.3	56±6
GroPIns4*P*	Genistein	0.29±0.06	22±16
PDGF	Genistein	0.19±4	5±3
ATP	Genistein	1.16±0.23***	78±5
GroPIns4*P*	SU6656/PP2	0.03±4	0
PDGF	SU6656/PP2	0.08±4	0
ATP	SU6656/PP2	0.75±0.3***	90±5

Cells were selected at random and scanned for at least 30 s to establish base-line fluorescence and to check for spontaneous $[Ca^{2+}]_i$ rises, then movies were taken over 8 min following the addition of the reported stimuli. For image analysis, the fluorescence of each frame was calculated by the TILL Photonics imaging system. The stimulation of $[Ca^{2+}]_i$ by 50 μM GroPIns4*P*, 10 ng/ml PDGF, 100 μM ATP, 10 μM ionomycin or 100 μM GroPIns was calculated as changes in fluorescence relative to base-line, as the pseudo-ratio: ΔF/F0=(F−F0)/(F0−B) where F is the maximal level of fluorescence obtained upon stimulation, F0 is the fluorescence under basal conditions, and B is the background [41,71,72]. Apart from changes that approach dye saturation, ΔF/F0 approximately reflects $[Ca^{2+}]_i$, assuming no changes in dye concentration, intracellular environment or path length [41,71,72]. The effects of 1 mM EGTA and of pretreatments with the inhibitors 5 μM U-73122 (PLC inhibitor; 10 min), 5 μM U-73443 (inactive analogue of PLC inhibitor; 10 min), 10 μM genistein (tyrosine-kinase inhibitor; 30 min), 10 μM SU6656 (Src inhibitor; 10 min) and 10 μM PP2 (Src inhibitor; 10 min) were tested. The number of responsive cells is given as the percentage of the total cells analyzed per sample. The data are means (±s.e.) of at least 12 independent experiments for GroPIns4*P* stimulation, and of at least 5 independent experiments for the other stimuli. w/o, without.
Statistical significance: ***$P<0.001$, compared to the untreated sample (paired Student's *t* test). w/o, no pretreatment.

Table 3
InsP_3 production in NIH3T3 cells

	Pretreatments	Treatments (% increase over control)		
		2 min	5 min	15 min
(a) Intact cells[a]				
GroPIns4*P*	w/o	22.0±4*	19.0±9*	nd
PDGF	w/o	37.0±19*	56.0±30*	nd
ATP	w/o	nd	72.5±29**	nd
Thrombin	w/o	nd	99.6±24**	nd
(b) Cell homogenates[b]				
GroPIns4*P*	w/o	0.7±17	28.0±16*	81.0±19*
GroPIns4*P*	Anti-PLCγ ab	nd	nd	13.7±12
GroPIns4*P*	Anti-PLCβ ab	nd	nd	64.0±33*
Thrombin	w/o	nd	31.0±4*	174.0±53**
Thrombin	Anti-PLCγ ab	nd	nd	158.0±32**
Thrombin	Anti-PLCβ ab	nd	nd	34.0±3**

Intact cells and cell homogenates (400 μg/sample) were treated with 50 μM GroPIns4*P*, 10 ng/ml PDGF, 100 μM ATP and/or 5 I.U./ml thrombin for the indicated times. The intracellular InsP_3 levels were quantified using a commercial kit (see Materials and methods). The data are means (±s.d.) of at least four independent experiments and are given as percentage increases over basal (untreated sample; as 100%). Where indicated, the quantification of InsP_3 production was carried out in the presence of the anti-PLCβ or anti-PLCγ antibodies (*ab*) (see Materials and methods). w/o, without.
Statistical significance: *$P<0.05$, **$P<0.01$, compared to the untreated sample (paired Student's *t* test). nd, not determined.
[a] Basal level of InsP_3 of 0.45±0.3 pmols/7×10^5 cells.
[b] Basal level of InsP_3 of 2.23±1.7 pmols/400 μg of homogenate.

(Table 2). To determine whether the opening of calcium channels in the plasma membrane contributed to these increases in $[Ca^{2+}]_i$, control experiments were performed in a Ca^{2+}-free buffer (containing 1 mM EGTA) [41,54]. Under these conditions, GroPIns4*P* addition still resulted in an increase in $[Ca^{2+}]_i$ that was similar to that induced in the presence of extracellular Ca^{2+}, thus excluding a contribution of Ca^{2+} influx in this GroPIns4*P*-stimulated response (Table 2). The contribution of phospholipase C (PLC) to this increase in $[Ca^{2+}]_i$ induced by GroPIns4*P* was then analyzed using the specific PLC inhibitor U-73122 (5 μM) [55]. U-73122 completely inhibited the GroPIns4*P*-dependent $[Ca^{2+}]_i$ increase, whereas the inactive analogue U-73443 (5 μM) did not (Table 2).

Altogether, these data support a role for PLC in the release of Ca^{2+} from intracellular stores driven by GroPIns4*P*, and indicate that this $[Ca^{2+}]_i$ increase should originate from PLC-mediated inositol 1,4,5-trisphosphate (InsP_3) formation. We thus directly evaluated InsP_3 production in NIH3T3 cells stimulated with both GroPIns4*P* (50 μM) and PDGF (10 ng/ml) (see Materials and methods). In intact cells, GroPIns4*P*-induced a 22% increase in InsP_3 within 2 min, similar to the effect of PDGF (37% increase) (Table 3).

We also analyzed the effects of the PLC inhibitor U-73122 [55] on GroPIns4*P*-induced ruffle formation. In serum-starved NIH3T3 cells, pretreated with 5 μM U-73122, GroPIns4*P*- and PDGF-dependent ruffle formation was inhibited by about 60% and 50%, respectively (Table 1). Again, the inactive U-73122 analogue (5 μM U-73343) was used in parallel as a control, and it did not prevent stimulation of ruffle formation by either GroPIns4*P* or PDGF, confirming the involvement of PLC in this process (Table 1).

Finally, we investigated which PLC isoform is involved in the GroPIns4*P*-dependent InsP_3 increase by selectively blocking PLCβ and PLCγ with specific antibodies (see Materials and methods) [42]. NIH3T3 cell homogenates were incubated with GroPIns4*P* for 15 min in the absence and presence of 20 μg/ml anti-PLCβ or anti-PLCγ antibodies [42]; the GroPIns4*P* stimulation of InsP_3 production was prevented by the anti-PLCγ antibody and partially reduced (by about 20%) by the anti-PLCβ antibody (Table 3). The selectivity of these antibodies was validated by stimulating cell homogenates with thrombin (5 I.U./ml), which, as expected, produced about a 175%

increase in InsP_3 that was blocked by the antibody raised against PLCβ, the specific PLC isoform coupled to the proteinase-activated receptor (PAR) family, but not by the anti-PLCγ antibody (Table 3) [56,57]. These data are consistent with GroPIns4*P* activating PLCγ, possibly via tyrosine-kinase-dependent phosphorylation. Indeed, an increase in tyrosine phosphorylation was detected on immunoprecipitated PLCγ upon addition of 50 μM GroPIns4*P* (as revealed by an antiphosphotyrosine antibody; see Materials and methods; data not shown). In addition, a 30 min treatment with the general tyrosine-kinase inhibitor genistein [58] greatly reduced the GroPIns4*P*-induced increase in $[Ca^{2+}]_i$ (Table 2).

In summary, the action of GroPIns4*P* on membrane ruffle formation is mediated by tyrosine-kinase-dependent phosphorylation that acts through PLCγ and $[Ca^{2+}]_i$ modulation.

3.5. GroPIns4P activates Src

PLCγ is a known substrate of the Src-family kinases [59,60]. Using the experimental approaches described above, specific inhibitors were used to verify whether these are the kinases specifically activated by GroPIns4*P*, and that lead to the phosphorylation and activation of PLCγ. Indeed, the Src-family kinase inhibitors SU6656 and PP2 (10 μM each) [61] completely prevented the $[Ca^{2+}]_i$ increase (Table 2) and reduced the formation of membrane ruffles induced by GroPIns4*P* in NIH3T3 cells (by 80% and 70%, respectively; Table 1).

The possibility that this GroPIns4*P* treatment of intact NIH3T3 cells induced the activation of Src kinases was then analyzed by Western blotting, using a specific antibody against the phosphorylated tyrosine 416 of Src (the site of Src autophosphorylation upon activation) [62,63] to reveal the levels of active Src (p-Src) present in this system (see Materials and methods). Upon treatment with GroPIns4*P*, there was an 80% increase in p-Src levels; this increase was rapid (15 s) and persisted for at least 2 min (Fig. 7A and B). Among the different Src isoforms, the 60-kDa band corresponding to c-Src (indicated throughout as Src) was the one modulated by GroPIns4*P* (Fig. 7B).

To determine whether this GroPIns4*P*-dependent activation of Src was due to the direct binding of GroPIns4*P* to Src itself, in-vitro Src kinase assays were performed with purified Src (see Materials and methods). Neither GroPIns4*P* per se nor GroPIns4*P* in combination with cell lysates (used as a supply of potential cofactors) activated Src. These data are consistent with the hypothesis that GroPIns4*P* activates Src (leading to ruffle formation) only in intact cells, and not in isolated systems. PMA (10 μM) applied as a positive control induced an expected activation of Src in the presence of cell lysate (about a 32% increase in the basal activity of Src, which was 0.64 ±0.02 pmoles phosphorylated peptide/minute).

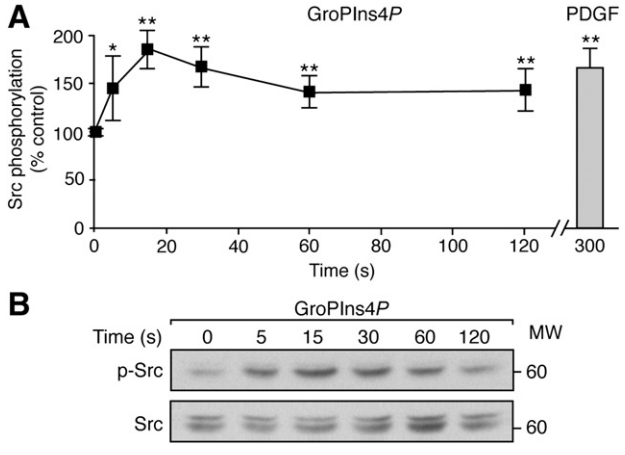

Fig. 7. GroPIns4*P*-dependent Src activation. Serum-starved NIH3T3 cells were stimulated with 50 μM GroPIns4*P* and/or 10 ng/ml PDGF for the indicated times. The cells were lysed and the amounts of active Src (p-Src, tyrosine-416-phosphorylated) were analysed by Western blotting and normalised for the total amount of c-Src in the lysates (see Materials and methods). (A) Quantification of Src phosphorylation, as indicated. Data are expressed as percentages of the unstimulated control, as means (±s.d.) of four independent experiments, each in duplicate. (B) Western blotting of a representative time course of GroPIns4*P*-induced Src activation. Upper panel, phosphorylated Src (*p-Src*); lower panel, total Src. Statistical significance: $*P<0.05$, $**P<0.01$, compared to the untreated time 0 controls (paired Student's *t* test). MW, molecular-weight marker (kDa).

To further investigate the involvement of Src kinases in GroPIns4*P*-dependent ruffle formation, we used SYF cells, which are widely used embryonic fibroblasts that do not express the three ubiquitously expressed Src isoforms: Src, Fyn and Yes [64]. First, the induction of membrane ruffles by GroPIns4*P* was analyzed following the protocols described above (see also Materials and methods). GroPIns4*P* did not induce ruffle formation in SYF cells, whereas PDGF and PMA, applied as controls, did (Fig. 8A and B). Importantly, after transfecting Src in SYF cells (see Materials and methods), the GroPIns4*P* effect was completely rescued, and produced a level 2.5-fold the control ruffle formation, clearly indicating that Src expression was sufficient to rescue the GroPIns4*P* action (Fig. 8C and D). The PDGF-induced ruffle formation in both wild-type SYF cells and after Src overexpression indicates that PDGF signalling in these SYF cells diverges from that of GroPIns4*P*.

In conclusion, the tyrosine-kinase Src is essential for GroPIns4*P*-induced membrane ruffling, both in NIH3T3 and SYF fibroblasts.

4. Discussion

In the present study, we delineate a novel signalling mechanism that is initiated by the phosphoinositide metabolite GroPIns4*P* and that leads to actin cytoskeleton reorganization in fibroblasts.

We show that in NIH3T3 cells GroPIns4*P* induces ruffle formation through a phosphorylation cascade involving Src, which phosphorylates and hence activates PLCγ [60,65]. This results in a $[Ca^{2+}]_i$ increase that triggers the activation of CaMKII, which can phosphorylate TIAM1 [48]. Once phosphorylated, TIAM1 translocates to the plasma membrane and binds Rac1, thus promoting ruffle formation (as schematized in Fig. 9).

Our data clearly demonstrate that the Src/Ca^{2+}/CaMKII pathway is essential for GroPIns4*P*-induced ruffle formation in NIH3T3 cells. The inhibition of both PLCs and Src kinases prevented the increase in $[Ca^{2+}]_i$ and consequently reduced ruffle formation; in addition, this GroPIns4*P* effect was completely inhibited in SYF cells that do not express Src.

An open question arising from these data concerns the mechanisms by which GroPIns4*P* activates Src. Src kinases are regulated by phosphorylation/de-phosphorylation events: Src kinase activation arises from the autophosphorylation of tyrosine 416, whereas phosphorylation of tyrosine 527 by the C-terminal Src kinase (CSK) blocks its activity [62]. Protein-tyrosine phosphatases, such as PTPα, Shp1 and Shp2, among others, remove the inhibitory phosphate (on tyrosine 527) and activate Src kinases [63]. Since we did not see any direct effect of GroPIns4*P* on Src, the possibility is that GroPIns4*P* either modulates Src kinase by interacting with one of its cofactors, or activates one of these specific Src phosphatases.

Besides the signalling cascade reported here, phosphorylated Src could also activate other effectors that are involved in ruffle formation. Vav, another specific exchange factor for Rac1, is a case in point, since it is ubiquitously expressed and its activation induces ruffle formation in fibroblasts [60,66]. Vav, however, is not activated upon GroPIns4*P* stimulation in NIH3T3 cells. This is at variance with Jurkat T-cells, where GroPIns4*P* induces Vav activation as a consequence of the inhibition of the adenylyl cyclase activity induced by GroPIns4*P*, which results in the activation of Lck (a member of the Src family) and, consequently

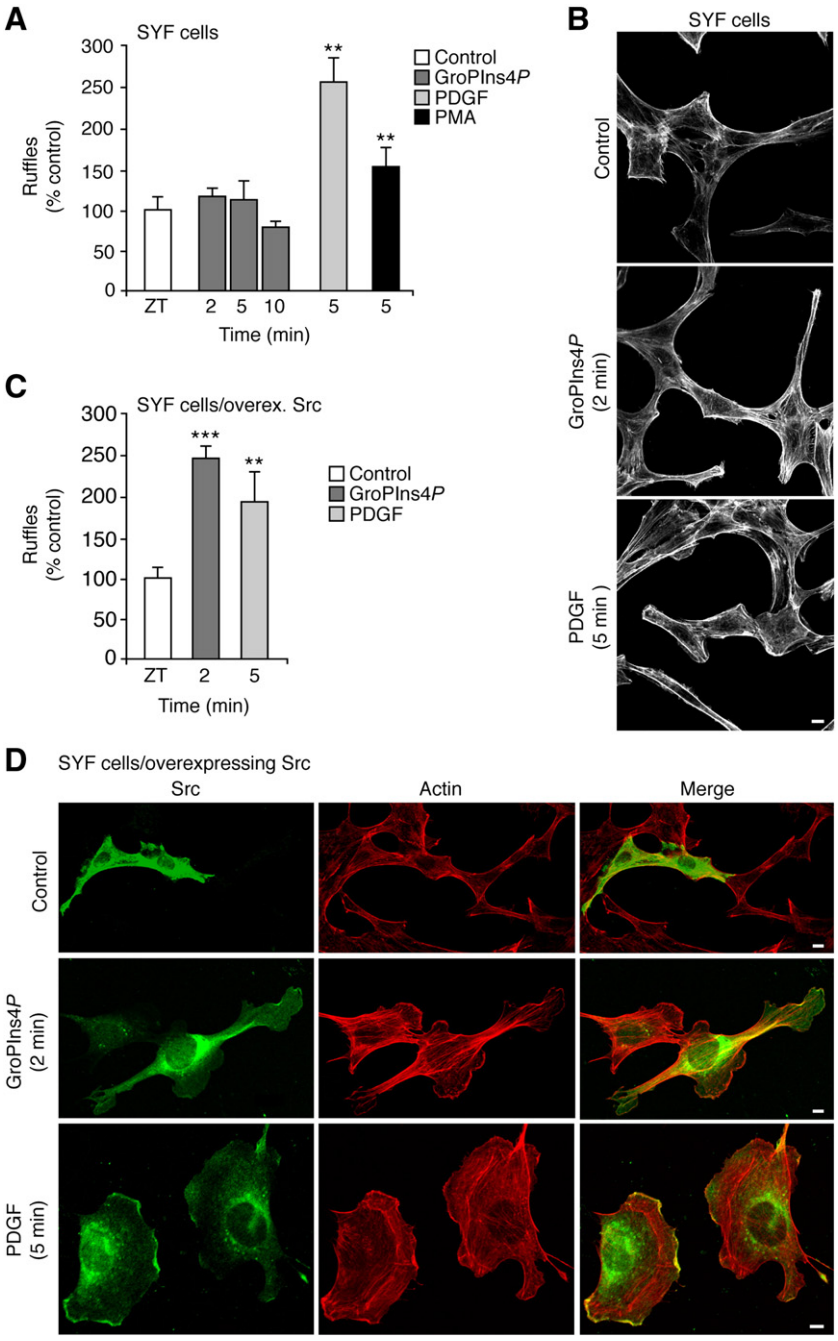

Fig. 8. GroPIns4*P*-dependent ruffle formation in SYF cells. Serum-starved SYF cells were stimulated with 50 μM GroPIns4*P*, 10 ng/ml PDGF or 10 μM PMA for the indicated times (see Materials and methods). Fixed cells were stained with TRITC-labelled phalloidin and analyzed by confocal microscopy. (A) Quantification of ruffle formation, as indicated (see Materials and methods). Data are expressed as percentages of the unstimulated ZT control, as means (±s.d.) of three independent experiments, each in duplicate. (B) Representative confocal images of actin staining, as indicated. Scale bar, 10 μm. (C) Quantification of ruffle formation in SYF cells overexpressing (*overex.*) Src and treated as indicated (see Materials and methods). Data are expressed as percentages of unstimulated ZT control, as means (±s.d.) of two independent experiments, each in duplicate. (D) Representative confocal images in cells overexpressing Src (green) showing actin staining (red), as indicated. Scale bars: 10 μm. Statistical significance: $^{**}P<0.01$ $^{***}P<0.001$ compared to the untreated ZT controls (paired Student's *t* test).

of Vav [13,14,67]. In NIH3T3 cells, the activation of TIAM1 does not involve adenylyl cyclase modulation: GroPIns4*P*-induced inhibition of the adenylyl cyclase in these cells was prevented by pertussis toxin treatment, a condition that did not affect GroPIns4*P*-induced ruffle formation, thus dissociating the Gi-protein/cAMP modulation from TIAM1 activation (Beatrice Maria Filippi, unpublished data). In conclusion, while the GroPIns4*P*-induced activation of both TIAM1 and Vav involves Src kinases, the mechanisms modulating the activity of these enzymes remain to be defined.

Another potential mechanism of action of GroPIns4*P* would involve its binding to specific membrane receptors. No experimental evidence has been obtained so far to support this hypothesis, despite a number of binding experiments performed using total membranes, plasma membranes, and intact and permeabilized cells (Beatrice Maria Filippi, unpublished data). GroPIns4*P* has instead been shown to permeate the cell membrane [68].

Our studies demonstrate that GroPIns4*P* is a multifunctional compound that can modulate different cell functions. While the

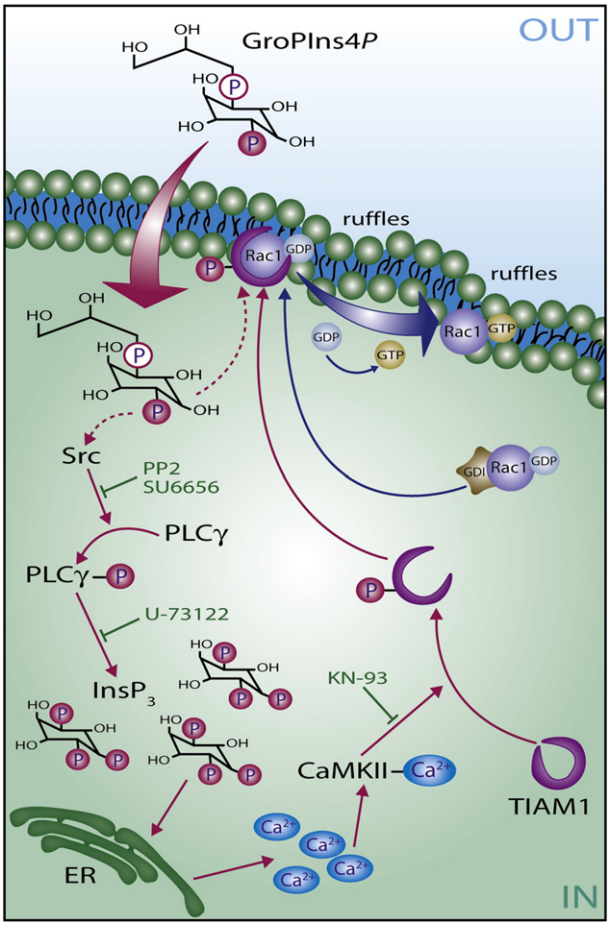

Fig. 9. Schematic representation of the pathway activated by GroPIns4*P* that leads to the induction of ruffle formation in NIH3T3 cells. GroPIns4*P* activates Src kinase, which phosphorylates and activates PLCγ, leading to the consequent InsP_3 production and $[Ca^{2+}]_i$ increase. This results in activation of CaMKII, which phosphorylates TIAM1, facilitating its translocation to the plasma membrane and enhancing its exchange activity versus Rac1. Once activated at the level of the plasma membrane, Rac1 promotes the formation of membrane ruffles. GDI indicates a generic Rac1 GDP dissociation inhibitor. See text for details.

present study focused on the effects and mechanisms of action of exogenously administered GroPIns4*P*, it should be stressed that the glycerophosphoinositols are present in virtually all cells [10] and that their intracellular levels can be increased by hormone stimulation via PLA_2 IVα activation [8]. This is the case also in fibroblasts, where GroPIns4*P* is formed upon growth-factor stimulation [7,67]. The basal physiological intracellular concentrations of GroPIns are in the low micromomolar range (about 50–450 μM), with GroPIns4*P* and glycerophosphoinositol 4,5-bisphosphate concentrations some 10-fold and 100-fold lower, respectively [10]; these are concentrations that are fully compatible with the effects studied by exogenous administration. In addition, the glycerophosphoinositols can permeate the plasma membrane, with kinetics compatible with the effects exerted when they are exogenously added to cultured cells [69]. Finally, by similar mechanisms, the glycerophosphoinositols can be released by cells that produce them at supra-physiological concentrations, and can act on proximal cell systems [13,68,69]. Altogether, these observations delineate a potential paracrine mechanism that in the case of GroPIns4*P* could be exerted by its hormone-induced release (for example, from leukocytes) [7], thus acting on target cells/tissues (fibroblasts in this case) under physiological conditions. More specifically, the recently reported GroPIns4*P* modulation of the chemotactic response in Jurkat T-cells and in peripheral blood lymphocytes may represent an example of its paracrine activity [13]. Thus, under physiological conditions an extracellular gradient arising from the GroPIns4*P* that is formed and released by macrophages in response to inflammatory stimuli and infection could activate T-cells, mediating the immune response in this way [13,70]. This potential role of the glycerophosphoinositols is presently under investigation.

Acknowledgements

We wish to thank M. Baldassare for the help in setting up the $[Ca^{2+}]_i$ measurements and the video imaging, M. Sallese for the help with experiments involving Src, and both M. Baldassare and M. Sallese together with A. Luini, R. Buccione and C.P. Berrie for their useful discussions, C. Iurisci for GroPIns4*P* preparation and technical assistance, I. Fleming (University of Dundee) for the TIAM1 constructs, J.G. Collard (The Netherlands Cancer Institute) for the anti-TIAM1 antibody, S. Gutkind (NIH, Bethesda) for the c-Src construct, A. Hall (Sloan-Kettering Institute for Cancer Research, NY) for the myc-tagged constitutively active forms of GTPases. E. Fontana for preparation of the Figures. and C.P. Berrie for the editorial assistance. We also acknowledge the financial support of Telethon Italia (Italy), the Italian Association for Cancer Research (AIRC, Milan, Italy), and the MIUR (Italy). B.M. Filippi and T. Pulvirenti were fellows of the Italian Foundation for Cancer Research (FIRC, Milan, Italy).

Appendix A. Supplementary data

Supplementary data associated with this article can be found, in the online version, at doi:10.1016/j.bbamcr.2008.07.021.

References

[1] S. Dowler, R.A. Currie, D.G. Campbell, M. Deak, G. Kular, C.P. Downes, D.R. Alessi, Identification of pleckstrin-homology-domain-containing proteins with novel phosphoinositide-binding specificities, Biochem. J. 351 (2000) 19–31.
[2] C.P. Downes, A. Gray, J.M. Lucocq, Probing phosphoinositide functions in signaling and membrane trafficking, Trends Cell Biol. 15 (2005) 259–268.
[3] C.P. Downes, A. Gray, A. Fairservice, S.T. Safrany, I.H. Batty, I. Fleming, The regulation of membrane to cytosol partitioning of signalling proteins by phosphoinositides and their soluble headgroups, Biochem. Soc. Trans. 33 (2005) 1303–1307.
[4] R.H. Michell, Inositol lipids in cellular signalling mechanisms, Trends Biochem. Sci. 17 (1992) 274–276.
[5] R.H. Michell, Evolution of the diverse biological roles of inositols, Biochem. Soc. Symp. (2007) 223–246.
[6] A. Toker, Phosphoinositides and signal transduction, Cell. Mol. Life Sci. 59 (2002) 761–779.
[7] D. Corda, C. Iurisci, C.P. Berrie, Biological activities and metabolism of the lysophosphoinositides and glycerophosphoinositols, Biochim. Biophys. Acta 1582 (2002) 52–69.
[8] S. Mariggiò, J. Sebastià, B.M. Filippi, C. Iurisci, C. Volonté, S. Amadio, V. De Falco, M. Santoro, D. Corda, A novel pathway of cell growth regulation mediated by a PLA_2α-derived phosphoinositide metabolite, FASEB J. 20 (2006) 2567–2569.
[9] S. Valitutti, P. Cucchi, G. Colletta, C. Di Filippo, D. Corda, Transformation by the k-ras oncogene correlates with increases in phospholipase A_2 activity, glycerophosphoinositol production and phosphoinositide synthesis in thyroid cells, Cell. Signal. 3 (1991) 321–332.
[10] C.P. Berrie, L.K. Dragani, J. van der Kaay, C. Iurisci, A. Brancaccio, D. Rotilio, D. Corda, Maintenance of PtdIns4,5P_2 pools under limiting inositol conditions, as assessed by liquid chromatography-tandem mass spectrometry and PtdIns4,5P_2 mass evaluation in Ras-transformed cells, Eur. J. Cancer 38 (2002) 2463–2475.
[11] S. Mariggiò, B.M. Filippi, C. Iurisci, L.K. Dragani, V. De Falco, M. Santoro, D. Corda, Cytosolic phospholipase A_2a regulates cell growth in RET/PTC-transformed thyroid cells, Cancer Res. 67 (2007) 11769–11778.
[12] R. Mancini, E. Piccolo, S. Mariggiò, B.M. Filippi, C. Iurisci, P. Pertile, C.P. Berrie, D. Corda, Reorganization of actin cytoskeleton by the phosphoinositide metabolite glycerophosphoinositol 4-phosphate, Mol. Biol. Cell 14 (2003) 503–515.
[13] L. Patrussi, S. Mariggiò, S.R. Paccani, N. Capitani, P. Zizza, D. Corda, C.T. Baldari, Glycerophosphoinositol-4-phosphate enhances SDF-1a-stimulated T-cell chemotaxis through PTK-dependent activation of Vav, Cell. Signal. 19 (2007) 2351–2360.
[14] L. Iacovelli, M. Falasca, S. Valitutti, D. D'Arcangelo, D. Corda, Glycerophosphoinositol 4-phosphate, a putative endogenous inhibitor of adenylylcyclase, J. Biol. Chem. 268 (1993) 20402–20407.
[15] C.M. Wells, P.J. Bhavsar, I.R. Evans, E. Vigorito, M. Turner, V. Tybulewicz, A.J. Ridley, Vav1 and Vav2 play different roles in macrophage migration and cytoskeletal organization, Exp. Cell Res. 310 (2005) 303–310.
[16] R. Buccione, M. Baldassarre, V. Trapani, C. Catalano, A. Pompeo, A. Brancaccio, R. Giavazzi, A. Luini, D. Corda, Glycerophosphoinositols inhibit the ability of tumour cells to invade the extracellular matrix, Eur. J. Cancer 41 (2005) 470–476.

[17] P. Keely, L. Parise, R. Juliano, Integrins and GTPases in tumour cell growth, motility and invasion, Trends Cell Biol. 8 (1998) 101–106.
[18] M. Mareel, A. Leroy, Clinical, cellular, and molecular aspects of cancer invasion, Physiol. Rev. 83 (2003) 337–376.
[19] C. Jimenez, R.A. Portela, M. Mellado, J.M. Rodriguez-Frade, J. Collard, A. Serrano, A.C. Martinez, J. Avila, A.C. Carrera, Role of the PI3K regulatory subunit in the control of actin organization and cell migration, J. Cell Biol. 151 (2000) 249–262.
[20] A. Obermeier, S. Ahmed, E. Manser, S.C. Yen, C. Hall, L. Lim, PAK promotes morphological changes by acting upstream of Rac, EMBO J. 17 (1998) 4328–4339.
[21] P. Timpson, G.E. Jones, M.C. Frame, V.G. Brunton, Coordination of cell polarization and migration by the Rho family GTPases requires Src tyrosine kinase activity, Curr. Biol. 11 (2001) 1836–1846.
[22] D. Brandt, M. Gimona, M. Hillmann, H. Haller, H. Mischak, Protein kinase C induces actin reorganization via a Src-and Rho-dependent pathway, J. Biol. Chem. 277 (2002) 20903–20910.
[23] Y.S. Bae, L.G. Cantley, C.S. Chen, S.R. Kim, K.S. Kwon, S.G. Rhee, Activation of phospholipase Cg by phosphatidylinositol 3,4,5-trisphosphate, J. Biol. Chem. 273 (1998) 4465–4469.
[24] T. Hirabayashi, T. Murayama, T. Shimizu, Regulatory mechanism and physiological role of cytosolic phospholipase A_2, Biol. Pharm. Bull. 27 (2004) 1168–1173.
[25] Y. Feng, C.A. Walsh, The many faces of filamin: a versatile molecular scaffold for cell motility and signalling, Nat. Cell Biol. 6 (2004) 1034–1038.
[26] J.V. Small, T. Stradal, E. Vignal, K. Rottner, The lamellipodium: where motility begins, Trends. Cell Biol. 12 (2002) 112–120.
[27] B.A. Connolly, J. Rice, L.A. Feig, R.J. Buchsbaum, Tiam1-IRSp53 complex formation directs specificity of Rac-mediated actin cytoskeleton regulation, Mol. Cell. Biol. 25 (2005) 4602–4614.
[28] P. Hahne, A. Sechi, S. Benesch, J.V. Small, Scar/WAVE is localised at the tips of protruding lamellipodia in living cells, FEBS Lett. 492 (2001) 215–220.
[29] A.J. Ridley, H.F. Paterson, C.L. Johnston, D. Diekmann, A. Hall, The small GTP-binding protein Rac regulates growth factor-induced membrane ruffling, Cell 70 (1992) 401–410.
[30] C.D. Nobes, A. Hall, Rho, Rac, and Cdc42 GTPases regulate the assembly of multimolecular focal complexes associated with actin stress fibers, lamellipodia, and filopodia, Cell 81 (1995) 53–62.
[31] J.T. Snyder, K.L. Rossman, M.A. Baumeister, W.M. Pruitt, D.P. Siderovski, C.J. Der, M.A. Lemmon, J. Sondek, Quantitative analysis of the effect of phosphoinositide interactions on the function of Dbl family proteins, J. Biol. Chem. 276 (2001) 45868–45875.
[32] R. Rohatgi, H.Y. Ho, M.W. Kirschner, Mechanism of N-WASP activation by CDC42 and phosphatidylinositol 4,5-bisphosphate, J. Cell Biol. 150 (2000) 1299–1310.
[33] I. Lassing, U. Lindberg, Specific interaction between phosphatidylinositol 4,5-bisphosphate and profilactin, Nature 314 (1985) 472–474.
[34] K. Barkalow, W. Witke, D.J. Kwiatkowski, J.H. Hartwig, Coordinated regulation of platelet actin filament barbed ends by gelsolin and capping protein, J. Cell Biol. 134 (1996) 389–399.
[35] P. Hilpela, M.K. Vartiainen, P. Lappalainen, Regulation of the actin cytoskeleton by PI(4,5)P_2 and PI(3,4,5)P_3, Curr. Top. Microbiol. Immunol. 282 (2004) 117–163.
[36] T. Takenawa, T. Itoh, Phosphoinositides, key molecules for regulation of actin cytoskeletal organization and membrane traffic from the plasma membrane, Biochim. Biophys. Acta 1533 (2001) 190–206.
[37] N.G. Clarke, R.M. Dawson, Alkaline O leads to N-transacylation. A new method for the quantitative deacylation of phospholipids, Biochem. J. 195 (1981) 301–306.
[38] F.G. Buchanan, C.M. Elliot, M. Gibbs, J.H. Exton, Translocation of the Rac1 guanine nucleotide exchange factor Tiam1 induced by platelet-derived growth factor and lysophosphatidic acid, J. Biol. Chem. 275 (2000) 9742–9748.
[39] A.J. Self, A. Hall, Measurement of intrinsic nucleotide exchange and GTP hydrolysis rates, Methods Enzymol. 256 (1995) 67–76.
[40] S. Moyano, J. Del Rio, D. Frechilla, Role of hippocampal CaMKII in serotonin 5-HT_{1A} receptor-mediated learning deficit in rats, Neuropsychopharmacology 29 (2004) 2216–2224.
[41] V.E. Klepeis, A. Cornell-Bell, V. Trinkaus-Randall, Growth factors but not gap junctions play a role in injury-induced Ca^{2+}waves in epithelial cells, J. Cell Sci. 114 (2001) 4185–4195.
[42] X. Ferry, V. Eichwald, L. Daeffler, Y. Landry, Activation of bg subunits of G_{i2} and G_{i3} proteins by basic secretagogues induces exocytosis through phospholipase Cb and arachidonate release through phospholipase Cg in mast cells, J. Immunol. 167 (2001) 4805–4813.
[43] R. Buccione, J.D. Orth, M.A. McNiven, Foot and mouth: podosomes, invadopodia and circular dorsal ruffles, Nat. Rev. Mol. Cell Biol. 5 (2004) 647–657.
[44] P. Sachdev, L. Zeng, L.H. Wang, Distinct role of phosphatidylinositol 3-kinase and Rho family GTPases in Vav3-induced cell transformation, cell motility, and morphological changes, J. Biol. Chem. 277 (2002) 17638–17648.
[45] L. Zeng, P. Sachdev, L. Yan, J.L. Chan, T. Trenkle, M. McClelland, J. Welsh, L.H. Wang, Vav3 mediates receptor protein tyrosine kinase signaling, regulates GTPase activity, modulates cell morphology, and induces cell transformation, Mol. Cell Biol. 20 (2000) 9212–9224.
[46] A.E. Mertens, R.C. Roovers, J.G. Collard, Regulation of Tiam1-Rac signalling, FEBS Lett. 546 (2003) 11–16.
[47] D.M. Pegtel, S.I. Ellenbroek, A.E. Mertens, R.A. van der Kammen, J. de Rooij, J.G. Collard, The Par-Tiam1 complex controls persistent migration by stabilizing microtubule-dependent front-rear polarity, Curr. Biol. 17 (2007) 1623–1634.
[48] I.N. Fleming, C.M. Elliott, F.G. Buchanan, C.P. Downes, J.H. Exton, Ca^{2+}/calmodulin-dependent protein kinase II regulates Tiam1 by reversible protein phosphorylation, J. Biol. Chem. 274 (1999) 12753–12758.
[49] M. Sumi, K. Kiuchi, T. Ishikawa, A. Ishii, M. Hagiwara, T. Nagatsu, H. Hidaka, The newly synthesized selective Ca^{2+}/calmodulin dependent protein kinase II inhibitor KN-93 reduces dopamine contents in PC12 h cells, Biochem. Biophys. Res. Commun. 181 (1991) 968–975.
[50] I.N. Fleming, C.M. Elliott, J.H. Exton, Phospholipase Cg, protein kinase C and Ca^{2+}/calmodulin-dependent protein kinase II are involved in platelet-derived growth factor-induced phosphorylation of Tiam1, FEBS Lett. 429 (1998) 229–233.
[51] A.J. Ridley, A. Hall, The small GTP-binding protein rho regulates the assembly of focal adhesions and actin stress fibers in response to growth factors, Cell 70 (1992) 389–399.
[52] L.S. Price, M. Langeslag, J.P. ten Klooster, P.L. Hordijk, K. Jalink, J.G. Collard, Calcium signaling regulates translocation and activation of Rac, J. Biol. Chem. 278 (2003) 39413–39421.
[53] A.P. Braun, H. Schulman, A non-selective cation current activated via the multifunctional Ca^{2+}-calmodulin-dependent protein kinase in human epithelial cells, J. Physiol. 488 (Pt 1) (1995) 37–55.
[54] S. Kuriyama, T. Ohuchi, N. Yoshimura, Y. Honda, Growth factor-induced cytosolic calcium ion transients in cultured human retinal pigment epithelial cells, Invest. Ophthalmol. Visual Sci. 32 (1991) 2882–2890.
[55] J.E. Bleasdale, N.R. Thakur, R.S. Gremban, G.L. Bundy, F.A. Fitzpatrick, R.J. Smith, S. Bunting, Selective inhibition of receptor-coupled phospholipase C-dependent processes in human platelets and polymorphonuclear neutrophils, J. Pharmacol. Exp. Ther. 255 (1990) 756–768.
[56] J.I. Hwang, K.J. Shin, Y.S. Oh, J.W. Choi, Z.W. Lee, D. Kim, K.S. Ha, H.S. Shin, S.H. Ryu, P.G. Suh, Phospholipase Cb3 mediates the thrombin-induced Ca^{2+}response in glial cells, Mol. Cells 19 (2005) 375–381.
[57] V.R. Vaidyula, A.K. Rao, Role of G aq and phospholipase Cb2 in human platelets activation by thrombin receptors PAR1 and PAR4: studies in human platelets deficient in Gαq and phospholipase Cb2, Br. J. Haematol 121 (2003) 491–496.
[58] T. Akiyama, J. Ishida, S. Nakagawa, H. Ogawara, S. Watanabe, N. Itoh, M. Shibuya, Y. Fukami, Genistein, a specific inhibitor of tyrosine-specific protein kinases, J. Biol. Chem. 262 (1987) 5592–5595.
[59] K. Sato, A.A. Tokmakov, T. Iwasaki, Y. Fukami, Tyrosine kinase-dependent activation of phospholipase Cg is required for calcium transient in Xenopus egg fertilization, Dev. Biol. 224 (2000) 453–469.
[60] E.T. Barfod, A.L. Moore, R.F. Melnick, S.D. Lidofsky, Src regulates distinct pathways for cell volume control through Vav and phospholipase Cg, J. Biol. Chem. 280 (2005) 25548–25557.
[61] J. Bain, H. McLauchlan, M. Elliott, P. Cohen, The specificities of protein kinase inhibitors: an update, Biochem. J. 371 (2003) 199–204.
[62] M.T. Brown, J.A. Cooper, Regulation, substrates and functions of Src, Biochim. Biophys. Acta 1287 (1996) 121–149.
[63] R. Roskoski Jr., Src protein-tyrosine kinase structure and regulation, Biochem. Biophys. Res. Commun. 324 (2004) 1155–1164.
[64] R.A. Klinghoffer, C. Sachsenmaier, J.A. Cooper, P. Soriano, Src family kinases are required for integrin but not PDGFR signal transduction, EMBO J. 18 (1999) 2459–2471.
[65] K. Shah, F. Vincent, Divergent roles of c-Src in controlling platelet-derived growth factor-dependent signaling in fibroblasts, Mol. Biol. Cell 16 (2005) 5418–5432.
[66] W.T. Arthur, L.A. Quilliam, J.A. Cooper, Rap1 promotes cell spreading by localizing Rac guanine nucleotide exchange factors, J. Cell Biol. 167 (2004) 111–122.
[67] M. Falasca, A. Carvelli, C. Iurisci, R.G. Qiu, M.H. Symons, D. Corda, Fast receptor-induced formation of glycerophosphoinositol-4-phosphate, a putative novel intracellular messenger in the Ras pathway, Mol. Biol. Cell 8 (1997) 443–453.
[68] C.P. Berrie, C. Iurisci, D. Corda, Membrane transport and in vitro metabolism of the Ras cascade messenger, glycerophosphoinositol 4-phosphate, Eur. J. Biochem. 266 (1999) 413–419.
[69] S. Mariggiò, C. Iurisci, J. Sebastià, J. Patton-Vogt, D. Corda, Molecular characterization of a glycerophosphoinositol transporter in mammalian cells, FEBS Lett. 580 (2006) 6789–6796.
[70] M.G. de Carvalho, J. Garritano, C.C. Leslie, Regulation of lysophospholipase activity of the 85-kDa phospholipase A_2 and activation in mouse peritoneal macrophages, J. Biol. Chem. 270 (1995) 20439–20446.
[71] A. Takahashi, P. Camacho, J.D. Lechleiter, B. Herman, Measurement of intracellular calcium, Physiol. Rev. 79 (1999) 1089–1125.
[72] K. Svoboda, W. Denk, D. Kleinfeld, D.W. Tank, In vivo dendritic calcium dynamics in neocortical pyramidal neurons, Nature 385 (1997) 161–165.